The Astrophysical Journal, 668:846–852, 2007 October 20

EVOLUTION OF FIELD SPIRAL GALAXIES UP TO REDSHIFTS $z = 1$[1]

Asmus Böhm[2,3] and Bodo L. Ziegler[2,4]

Received 2006 January 12; accepted 2007 June 26

ABSTRACT

We have gained intermediate-resolution spectroscopy with the FORS instruments of the Very Large Telescope (VLT) and high-resolution imaging with the Advanced Camera for Surveys aboard *HST* for a sample of 220 distant field spiral galaxies within the FORS Deep Field and William Herschel Deep Field. Spatially resolved rotation curves were extracted and fitted with synthetic velocity fields that take into account all geometric and observational effects, such as blurring due to the slit width and seeing influence. Using these fits, the maximum rotation velocity $V_{\max}$ could be determined for 124 galaxies that cover the redshift range $0.1 < z < 1.0$ and comprise a variety of morphologies from early-type spirals to very late types and irregulars. The luminosity-rotation velocity distribution of this sample, which represents an average look-back time of $\sim$5 Gyr, is offset from the Tully-Fisher relation (TFR) of local low-mass spirals, whereas the distant high-mass spirals are compatible with the local TFR. Taking the magnitude-limited character of our sample into account, we show that the slope of the local and the intermediate-z TFR would be in compliance if its scatter decreased by more than a factor of 3 between $z \approx 0.5$ and 0. Accepting this large evolution of the TFR scatter, we hence find no strong evidence for a mass- or luminosity-dependent evolution of disk galaxies. On the other hand, we derive stellar mass-to-luminosity ratios (M/L) that indicate a luminosity-dependent evolution in the sense that distant low-luminosity disks have much lower M/L than their local counterparts, while high-luminosity disks barely evolved in M/L over the covered redshift range. This could be the manifestation of the "downsizing" effect, i.e., the successive shift of the peak of star formation from high-mass to low-mass galaxies toward lower redshifts. This trend might be canceled out in the TF diagram due to the simultaneous evolution of multiple parameters. We also estimate the ratios between stellar and total masses, finding that these remained constant since $z = 1$, as would be expected in the context of hierarchically growing structure.

Subject headings: galaxies: evolution — galaxies: kinematics and dynamics — galaxies: spiral

Online material: color figures

1. INTRODUCTION

The concept of cold dark matter (CDM) and its prediction of hierarchical structure growth has become an astrophysical paradigm in the last decade. Observations of the cosmic microwave background (e.g., Spergel et al. 2003) or the large-scale structure (e.g., Bahcall et al. 1999) strongly support the idea that the vast majority of matter is nonbaryonic, nonluminous, and interacts only gravitationally. In this picture, gas and stars are embedded in dark matter halos, and low-mass systems were the first virialized structures in the early cosmic stages, followed by an epoch of accretion and merger events during which larger systems were successively built up. Disks are destroyed during the frequent mergers of similar-mass galaxies at $z > 1$, but can regrow via accretion events at lower redshifts (e.g., Abadi et al. 2003).

An important tool for the quantitative test of the predictions from numerical simulations based on the hierarchical scenario are scaling relations that link galaxy parameters. Within the last years, several studies focused on the evolution of such relations up to redshifts $z \approx 1$, corresponding to more than half the age of the universe, or even beyond. Many analyses utilized the Tully-Fisher relation (TFR) between the maximum rotation velocity $V_{\max}$ and the luminosity or stellar mass (e.g., Vogt 2001; Ziegler et al. 2002; Milvang-Jensen et al. 2003; Böhm et al. 2004; Bamford et al. 2006; Conselice et al. 2005; Flores et al. 2006; Nakamura et al. 2006; Weiner et al. 2006; Chiu et al. 2007; Kassin et al. 2007).

Studies focusing on the stellar mass TFR have consistently found no evidence for evolution over the past $\sim$7 Gyr (e.g., Conselice et al. 2005; Kassin et al. 2007). On the other hand, analyses exploiting the rest-frame B-band TFR—which is less sensitive to the stellar mass than to the fraction of young stars—yielded quite discrepant results. This is somewhat surprising, since most recent TFR studies comprise $\sim$100 objects or more. Some authors derived much higher luminosities of spiral galaxies in the past (e.g., Böhm et al. 2004; Bamford et al. 2006; Chiu et al. 2007), while others find only a very modest evolution in luminosity (e.g., Vogt 2001; Flores et al. 2006). There is also still debate as to whether the B-band TFR changes its slope with redshift, which would imply an evolution depending on $V_{\max}$ and hence on total galaxy mass. In Böhm et al. (2004, hereafter B04), we found that low-mass spirals at $\langle z \rangle \approx 0.5$ were brighter by up to several magnitudes than in the local universe, while high-mass spirals barely evolved in M_B at given $V_{\max}$. On the other hand, Weiner et al. (2006) observe a stronger brightening in the high-mass than in the low-mass regime toward larger redshifts. From the theoretical side, the situation is similarly unclear: in some simulations, the B-band TFR slope remains constant with look-back time and only the magnitude zero point changes (e.g., Steinmetz & Navarro 1999; Portinari & Sommer-Larsen 2007), while an evolution in slope is predicted by other authors (e.g., Boissier & Prantzos 2001; Ferreras & Silk 2001).

[1] Based on observations collected at the European Southern Observatory, Cerro Paranal, Chile (ESO nos. 65.O-0049, 66.A-0547, 68.A-0013, 69.B-0278B, and 70.B-0251A) and observations with the NASA/ESA *Hubble Space Telescope*, PID 9502 and 9908.

[2] Institut für Astrophysik Göttingen, Friedrich-Hund-Platz 1, 37077 Göttingen, Germany; boehm@astro.physik.uni-goettingen.de, bziegler@astro.physik.uni-goettingen.de

[3] Astrophysikalisches Institut Potsdam, An der Sternwarte 16, 14482 Potsdam, Germany; aboehm@aip.de

[4] Argelander-Institut für Astronomie, Auf dem Hügel 71, 53121 Bonn, Germany.

A growing number of observational studies based on methods other than the TFR have pointed toward a mass-dependent evolution of distant galaxies, in terms either of their colors (e.g., Kodama et al. 2004), mass-to-light ratios (e.g., van der Wel et al. 2005), or average stellar ages (e.g., Ferreras et al. 2004). These results indicate that the global stellar populations of distant high-mass galaxies are on average older than those of distant low-mass galaxies, similar to what has been found in the local universe (e.g., Bell & de Jong 2000). Since small galaxies are understood as ancient building blocks within the framework of hierarchical structure growth, and in turn should have an older stellar content than larger systems formed more recently, these observations are at variance with the straightforward expectation. They can be interpreted such that the peak of star formation shifts from high-mass to low-mass galaxies with growing cosmic age, a phenomenon that was termed "downsizing" by Cowie et al. (1996). It is, however, a nontrivial question what kind of imprint "downsizing" has on the TFR, since the luminosity-$V_{\rm max}$ diagram most likely probes the evolution of various galaxy properties simultaneously, including stellar M/L, gas mass fraction, dust content, etc.

In this paper, we report on an extensive observational study of spiral galaxy evolution over the last 7 Gyr. The new sample holds 124 intermediate-z disk galaxies with reliable $V_{\rm max}$ measurements, roughly doubling the size of our previous data set from B04. The analysis given therein was limited to ground-based imaging, while here we can rely on our high-resolution imaging performed with the Advanced Camera for Surveys of the *HST*. This allows a much more accurate determination of disk inclination angles, scale lengths, etc., and in turn a more robust estimate of the maximum rotation velocities. Extending the approach used in B04, we will analyze the evolution not only of the TFR but also of the stellar mass-to-light ratios and the stellar mass fractions. We stress that this is the first refereed publication on the total sample; only some brief excerpts were shown in Ziegler et al. (2006).

The structure of this paper is as follows. In § 2, we describe the target selection, spectroscopic data reduction, and redshift determination. Section 3 briefly introduces the *HST*/ACS imaging and morphological analysis. Details on the derivation of the intrinsic maximum rotation velocities and luminosities are given in § 4. We present and discuss our results in § 5, followed by a short summary in § 6. Throughout this article we assume a flat cosmology with $\Omega_\lambda = 0.7$, $\Omega_m = 0.3$, and $H_0 = 70$ km s^{-1} Mpc^{-1}.

2. VLT SPECTROSCOPY

We selected our targets utilizing the multiband photometric surveys in the FORS Deep Field (FDF; Heidt et al. 2003) and William Herschel Deep Field (WHDF; Metcalfe et al. 2001). Note that the sample used in B04 comprised only FDF data. The following criteria were applied: (1) total apparent brightness $R <$ 23 mag; (2) spectrophotometric type "later" than Sa, based on a photometric redshift catalog in the case of the FDF (see Bender et al. 2001) or color-color diagrams for the WHDF objects (no photometric redshifts were available for these), adopting the evolutionary tracks given in Metcalfe et al. (2001); (3) disk inclination angle $i > 40^\circ$ and misalignment angle between apparent major axis and slit direction $\delta < 15^\circ$. The two latter constraints were chosen to limit the geometric distortions of the observed rotation curves. Apart from these limits, our selection was morphologically "blind." No selection on emission line strength was performed.

Using the FORS 1 and 2 instruments of the VLT in multi-object spectroscopy (MOS) mode, we took spectra of a total of 220 late-type galaxies between 2000 September and 2002 October. In the MOS masks, we also included a total of ~40 early-type galaxies for a different study (see Ziegler et al. 2005). If a target initially selected as an E/S0 galaxy turned out to have the spectrum of an early-type spiral (Sa/Sab), it was included in the disk galaxy sample a posteriori. Such a strategy helps to avoid selection biases against high M/L.

We used a fixed slit width of 1.0″, which resulted in spectral resolutions of $R \approx 1200$ for the FDF observations, where the grism 600*R* was used, and $R \approx 1000$ in the WHDF with the grism 600*RI*. Each setup was exposed for a total of 2.5 hr under seeing conditions between 0.43″ and 0.92″ FWHM, with a median of 0.76″. The spatial sampling in the final spectra was 0.2″ pixel^{-1} (FDF) and 0.25″ pixel^{-1} (WHDF, after the FORS 2 CCD upgrade).

The data reduction was conducted on single extracted spectra. All reduction steps were performed on the individual exposures before they were finally combined. The typical rms of the dispersion relation fitted for wavelength calibration was 0.04 Å. For 202 of the galaxies, a redshift determination and spectral classification was feasible. The objects range from $z = 0.03$ to 1.49 with a median $\langle z \rangle = 0.43$ (the redshift distribution of the final sample entering the Tully-Fisher analysis is given in § 4).

3. *HST*/ACS IMAGING

The *HST*/ACS observations were carried out during cycles 11 and 12. To cover the 6×6 arcmin^2 sky areas of the FORS and William Herschel Deep Fields, 2×2 mosaics were taken with the Wide Field Camera that has a field of view of $\sim 200 \times 200$ arcsec^2 and a pixel scale of 0.05″. Four visits, each with a total exposure time of 2360 s (FDF) and 2250 s (WHDF) through the F814W filter, were used per quadrant. Each visit was split into two exposures. We kept the resulting frames from the ACS pipeline reduction (including bias subtraction, flat-fielding, and distortion correction) and used a filtering algorithm to combine the two exposures of each visit and remove the cosmics.

The structural parameters of the galaxies were derived with the GALFIT package (Peng et al. 2002). For convolution of the model profiles, a mean point-spread function (PSF) was constructed using ~20 unsaturated stars with $I_{814} < 23$, which were normalized to the same central flux and median averaged. An exponential profile was used to fit the galaxies' disk components, while a Sérsic profile was taken to model an additional bulge, where detectable. Note that for the analysis presented here, the most important parameters are the inclination, position angle, and scale length of the disk. The best-fitting bulge parameters were only used for a raw morphological classification.

We found significant bulge components in only 46 out of 124 galaxies that were reliable for $V_{\rm max}$ determination (see § 4), spanning the range $0.01 \leq B/T \leq 0.53$ (median $\langle B/T \rangle = 0.15$). In terms of a visual classification within the Hubble scheme, our sample comprises all types from Sa spirals to irregulars.

4. TULLY-FISHER PARAMETERS

To extract rotation curves (RCs) from the two-dimensional (2D) spectra, Gaussian fits were applied to the emission lines stepwise perpendicular to the direction of dispersion. An averaging boxcar of three pixel widths, corresponding to 0.6″, was used to increase the signal-to-noise ratio (S/N). For very weak lines, this boxcar size was increased to five pixels. In cases of multiple usable emission lines for a given object, the RC with the largest spatial extent and highest degree of symmetry was used as reference. RCs from different emission lines agreed within the errors (at least in terms of the derived maximum rotation velocities) for the majority of the objects. Most of the "reference" RCs were extracted from the [O II] or [O III] lines, a smaller fraction from

Hα or Hβ (for a vast number of example rotation curves, please see B04).

Due to the small apparent sizes of the spirals in our sample, the observed rotation curves were heavily blurred. At redshifts of $z \approx 0.5$, the apparent scale lengths are of the same order as the slit width (1″ for the entire data set) and the seeing disk. The maximum rotation velocity hence cannot be derived straightforwardly from the outer regions of the observed rotation curves.

To account for the blurring effects, we generated synthetic rotation velocity fields according to the measured disk inclination, position angle, and scale length of a given object. We assumed an intrinsic linear rise of the rotation velocity at small radii, which turns over into a regime of constant rotation velocity at large radii, with the turnover radius computed from the scale length of the emitting gas (for details on this prescription as well as tests of various rotation curve shapes, we again refer the reader to B04). Using the position angle and disk inclination derived with GALFIT, a 2D rotation velocity field was generated. After weighting with the luminosity profile and convolution with the PSF, a "stripe" was extracted from the velocity field that corresponded to the orientation and width of the given slitlet used for spectroscopy. This simulation yielded a *synthetic* rotation curve, which was fitted to the corresponding observed curve to derive the intrinsic value of $V_{\rm max}$.

Following this approach, $V_{\rm max}$ values could be determined for 124 spirals in our sample (hereafter, we refer to this kinematic data set as the TF sample). Of these 78 galaxies were rejected, partly due to disturbed kinematics, which could introduce systematic errors in the TF analysis. Other objects were not suitable due to low-S/N, solid-body rotation, or the lack of significant rotation within the measurement errors. The TF sample galaxies span the redshift range $0.05 < z < 0.97$ (median 0.45, corresponding to a look-back time of 4.7 Gyr) and comprise 19 objects with spectrophotometric type Sab, 65 Sc spirals, and 40 Sdm galaxies. The $V_{\rm max}$ values fall in the range of 22 km s^{-1} $< V_{\rm max} <$ 450 km s^{-1} (median $\langle V_{\rm max}\rangle = 135$ km s^{-1}).

The computation of the luminosities benefitted strongly from the multiband imaging of our targets. Depending on the redshift of a given object, the filter which best matched the rest-frame B band was used to compute the absolute magnitude M_B. This way, systematic k-correction errors due to dependence on the SED are very small (<0.1 mag for all types and redshifts in our data set). Intrinsic absorption was corrected following Tully & Fouqué (1985). In this approach, the amount of absorption only depends on the disk inclination. For testing purposes, we alternatively applied the inclination- *and* mass-dependent correction factors given by Tully et al. (1998). However, this did not change the results presented here. It only is crucial that any distant sample is corrected for internal absorption *in the same way* as the local sample it is compared to. Since we use the data from Pierce & Tully (1992), who adopted the Tully & Fouqué approach, as local reference here, we will keep this convention in the following discussion. The TF galaxies have absorption-corrected absolute magnitudes between $M_B = -16.8$ and -22.7 (median $\langle M_B\rangle = -20.3$). The 78 galaxies with RCs that were not reliable for a $V_{\rm max}$ determination have slightly lower luminosities, with a range of $-22.4 < M_B < -14.8$ and a median value of $\langle M_B\rangle = -19.8$.

In Figure 1 we compare our sample to the local Tully-Fisher relation from Pierce & Tully (1992, hereafter PT92). On average, the FDF and WHDF spirals are more luminous than their local counterparts by $\langle \Delta M_B\rangle = -0.84$ mag, which could be due to younger stellar populations, i.e., lower M/L of the distant galaxies. This interpretation is supported by the fact that the amount

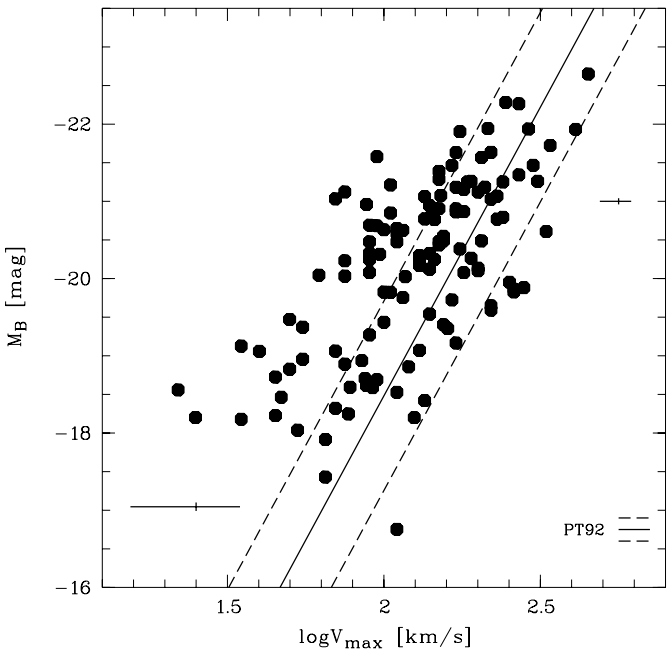

FIG. 1.—Distant FDF and WHDF galaxies at $\langle z\rangle = 0.45$ compared to the local Tully-Fisher relation as given by Pierce & Tully (1992, *solid line*; the dashed lines denote the 3 σ limits). The distant spirals are systematically overluminous for their values of $V_{\rm max}$. Typical error bars for the high-mass and low-mass regime are indicated in the upper-right and lower-left corner, respectively.

of the distant galaxies' brightening, ΔM_B, increases with redshift. A linear χ^2 fit yields $\Delta M_B = (-1.22 \pm 0.40)z - (0.02 \pm 0.20)$ mag. Here, we took the error propagation of $V_{\rm max}$ errors as well as the typical errors for the local spirals into account. This luminosity evolution is in agreement with the findings by, e.g., Milvang-Jensen et al. (2003), but exceeds the very modest TF offsets derived by Vogt (2001).

5. DISCUSSION

The luminosity-rotation velocity distribution of our sample indicates that the offsets from the local Tully-Fisher relation change not only with redshift (see above) but also with mass: while the high-mass spirals are in relatively good agreement with the local TFR, the low-mass spirals are overluminous by up to several magnitudes at given $V_{\rm max}$ (cf. Fig. 1). Using a 100 iteration bootstrap bisector fit, we find an intermediate-redshift TFR of $M_B = -(4.27 \pm 0.30) \log V_{\rm max} - (11.18 \pm 0.65)$, which is a significantly shallower slope ($a = -4.27$) than locally, where $a = -7.48$ is observed (PT92); we emphasize that this published value is in good agreement with a bisector fit to the local sample, which yields $a = -7.57 \pm 0.38$. Note that the bisector fitting method, which is a combination of a "forward" and an "inverse" TF fit, can be only weakly affected by potentially correlated errors in ΔM_B and $V_{\rm max}$ suspected by Bamford et al. (2006).

We reported earlier on a potential mass-dependent luminosity evolution with an analysis that was limited to the FDF subsample and ground-based structural parameters (Ziegler et al. 2002; B04). There, we ruled out a variety of systematic errors that potentially could bias the observed distant TFR slope. First, we tested whether tidally induced star formation in close galaxy pairs affects our sample, but found that the TF distributions of pair candidates and isolated galaxies are consistent. Second, our results were robust against the use of different prescriptions for the intrinsic absorption correction. Third, we subdivided the FDF sample according to the rotation curve quality in terms of radial extent and symmetry.

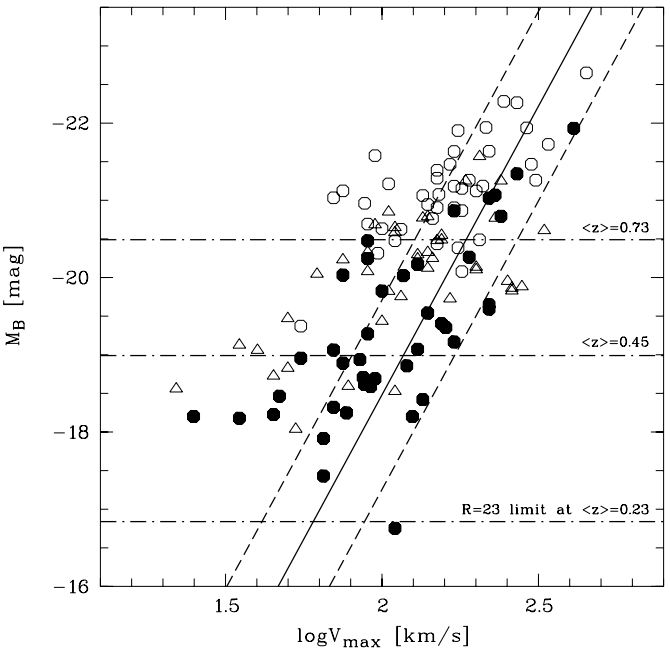

FIG. 2.—FDF and WHDF galaxies compared to the local TFR as given by Pierce & Tully (1992, *solid line*; the dashed lines denote the 3 σ limits). The distant sample is divided into three equally sized sets with median redshifts $\langle z\rangle = 0.23$ (*filled circles*), $\langle z\rangle = 0.45$ (*open triangles*), and $\langle z\rangle = 0.73$ (*open circles*). The horizontal dot-dashed lines depict the limit in *B*-band absolute magnitude corresponding to our selection on apparent brightness $R < 23$ mag. An SED corresponding to Hubble type Sc has been assumed here. [*See the electronic edition of the Journal for a color version of this figure.*]

A reanalysis using only high-quality rotation curves confirmed the shallower distant TF slope, showing that our findings are not induced by perturbated or truncated rotation curves.

We also tested whether a slope change could be mimicked by an incompleteness effect arising from the apparent magnitude limit in our target selection. Toward higher redshifts, such a limit corresponds to higher luminosities and in turn higher masses. A fraction of the low-luminosity, low-mass (slowly rotating) spiral population is therefore missed in the selection process, while the low-mass galaxies that *are* selected might preferentially be located at the high-luminosity side of the relation.

To test this effect on the new, full sample, we split it into three equally sized redshift bins corresponding to median redshifts $\langle z\rangle = 0.23$, $\langle z\rangle = 0.45$, and $\langle z\rangle = 0.73$ (see Fig. 2). In all redshifts bins, at a given $V_{\rm max}$ the distant galaxy sample shows an overluminosity of the low-mass galaxies compared to the local TFR, while the distributions are similar at the high-mass end. Using bootstrap bisector fits, we find significant deviations from the local TFR slope in all redshift bins: $a = -4.18 \pm 0.35$ at $\langle z\rangle = 0.23$, $a = -2.77 \pm 0.56$ at $\langle z\rangle = 0.45$, and $a = -3.00 \pm 0.50$ at $\langle z\rangle = 0.73$. Also shown in Figure 2 are the absolute magnitudes to which our selection criterion $R < 23$ mag corresponds at the median redshift of each subsample (*dot-dashed lines*). To derive these limits, we computed the *k*-correction using a synthetic spectrum of type Sc by Möller et al. (2001). Note that the *k*-correction for transformation from $R_{\rm obs}$ to $B_{\rm rest}$ is only weakly dependent on SED type at redshifts $0.3 \lesssim z \lesssim 0.8$. To achieve consistency, we corrected for intrinsic absorption at a disk inclination angle of $i = 60^\circ$, which is the average of our data set. It is evident from Figure 2 that the magnitude limit of our survey affects the covered luminosity ranges in the intermediate- and high-redshift bin. In the low-redshift bin ($\langle z\rangle = 0.23$), the lack of galaxies with $M_B \gtrsim -18$ seems less likely to be induced by the $R < 23$ mag selection. In the following, we aim at a quantitative estimate of the impact of sample incompleteness on the TF analysis.

The key factor for the strength of this selection effect is the scatter of the TFR, which has a value of $\sigma_B = 0.41$ mag in the *B* band of the local PT92 sample. In a previous analysis (Ziegler et al. 2002), we assumed that this scatter increases by a factor of 1.5 between $z \approx 0$ and $z = 0.5$ due to, e.g., a broader distribution in star formation rates at earlier comic stages. Here, we will use a different approach by testing *how strongly the TF scatter would have to evolve over the past* $\sim$5 Gyr *for the* $V_{\rm max}$*-dependent TF offsets to be attributed to an incompleteness effect*.

We hence assumed that the slope of the TFR remained constant over the redshift range under scrutiny here, and that its scatter has been larger at earlier cosmic times. Similar to the technique described by Giovanelli et al. (1997), a Schechter luminosity function (LF) form was fitted to the observed luminosity distribution, with the characteristic luminosity M^* and the space density ϕ^* as free parameters. At the faint end of the luminosity function, where our sample is incomplete, a slope of $\alpha = -1.2$ was adopted, which is a typical value found in studies of the *B*-band LF at intermediate redshifts (e.g., Gabasch et al. 2004; Giallongo et al. 2005). We could not determine the faint-end slope directly from the data, since the luminosity distribution of our sample peaks at $M_B \approx -20$ and falls off toward fainter magnitudes due to incompleteness. The ratio between the observed LF and the best-fit Schechter LF was computed and expressed as an incompleteness function $y = f(M_B)$ that ranged from $y = 1$ in the case of 100% completeness to $y = 0$ in the case of 0% completeness. On the basis of the local TFR, $y = f(M_B)$ was then converted to $y = f(V_{\rm max})$. This was done because the distribution in $V_{\rm max}$ is much less affected by the apparent magnitude limit than the distribution in M_B; hence, the incompleteness bias was computed as a function of $V_{\rm max}$, not as a function of M_B.

To derive the impact of the sample incompleteness, an *unbiased* TFR of the form $M_B = a \log V_{\rm max} + b$ was assumed with a fixed slope $a = -7.48$. The TFR intercept b was determined implicitely from the best-fit value of the characteristic luminosity M^*. We stress again that the purpose of this approach was only to test whether a time-independent TF slope could be consistent with our data set. For each object in the TF sample with an *observed* maximum rotation velocity $V_{\rm max}$, the incompleteness function $y = f(V_{\rm max})$ was taken as the probability that the given galaxy would enter the observed TF sample with an observed, biased absolute magnitude $M_B^b = a \log V_{\rm max} + b \pm \sigma(V_{\rm max})$. As observed in the local universe (e.g., Giovanelli et al. 1997), the scatter $\sigma(V_{\rm max})$ was assumed to be larger for lower mass galaxies (at, e.g., $V_{\rm max} = 100$ km s^{-1}, the scatter was taken to be a factor of 1.6 larger than at $V_{\rm max} = 300$ km s^{-1}) with an average value satisfying $\langle \sigma(V_{\rm max})\rangle = \sigma_B$. This computation of M_B including a TF scatter was iterated 800 times for every object, yielding a simulated, *biased* TF relation. The difference between the absolute magnitude $M_B = f(V_{\rm max})$ of the unbiased TFR and the simulated absolute magnitude $M_B^b = f(V_{\rm max})$ of the biased TFR was taken as the *correction factor* to debias our TF sample. Note that the debiased magnitudes $M_B^{\rm db}$ are fainter than the observed values, and that the TFR becomes steeper after debiasing.

These computations were performed in three variants using (1) the local scatter σ_B, (2) a 2 $\times$ local scatter, and (3) a 3 $\times$ local scatter for the intermediate-*z* TFR. The corresponding debiased TF samples were fitted with bootstrap bisector fits. To account for the fact that the distant galaxies cover a range in redshift, corresponding to various lookback times, the multiplication factor for introducing the scatter in the simulated distant TFR was not kept

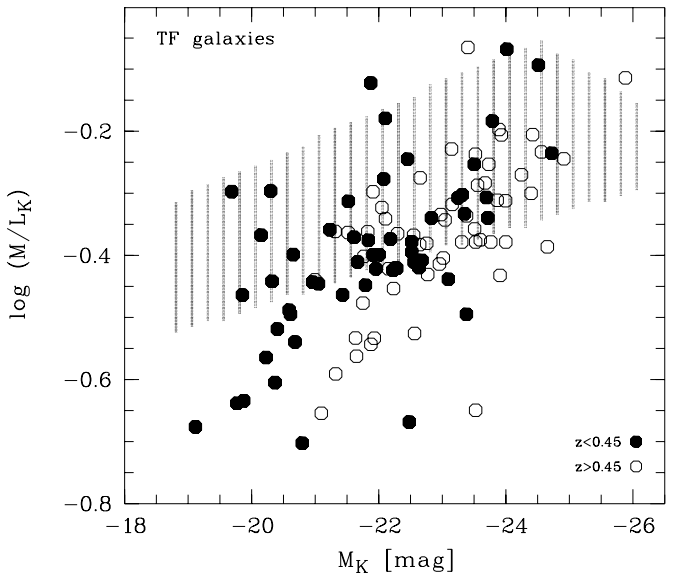

FIG. 3.—Stellar mass-to-light ratios of our distant TF sample galaxies at $0.1 < z < 0.45$ (*filled circles*) and $0.45 < z < 1.0$ (*open circles*), compared to the parameter range covered by present-day spirals (*shaded area*) from Bell & de Jong (2001). The data indicate a stronger evolution in M/L for low-luminosity galaxies. [*See the electronic edition of the Journal for a color version of this figure.*]

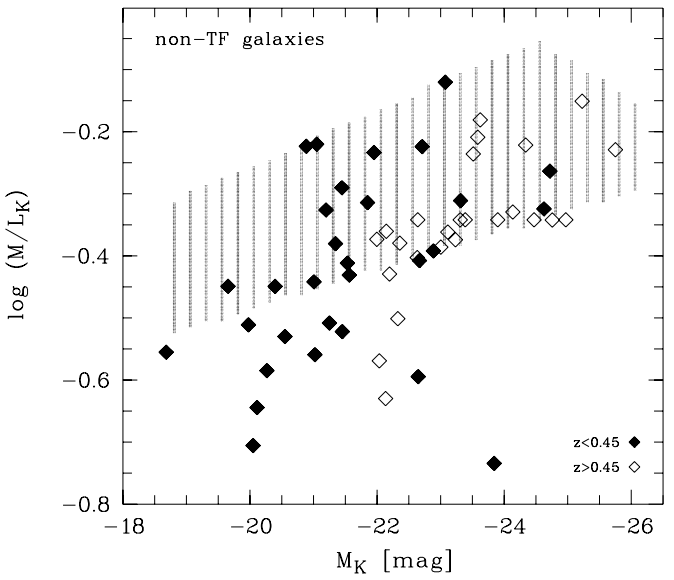

FIG. 4.—Stellar mass-to-light ratios of the distant galaxies that were not usable for a determination of $V_{\max}$, split into two redshift bins for $0.1 < z < 0.45$ (*filled diamonds*) and $0.45 < z < 1.0$ (*open diamonds*). The parameter range covered by present-day spirals from Bell & de Jong (2001) is indicated by the shaded area. Similar as for the TF objects (see Fig. 3), the data indicate a stronger evolution in M/L for low-luminosity galaxies. [*See the electronic edition of the Journal for a color version of this figure.*]

constant for the whole sample but computed individually for each object in such a way that the *average* scatter was either equal to σ_B, 2 σ_B, or 3 σ_B.

Using this approach, we found that the unbiased distant TFR slope would be $a = -4.88 \pm 0.29$ if the distant TF scatter was the same as locally. If the scatter doubles between $z = 0$ and $z \sim 0.5$, the incompleteness effect becomes stronger, and the debiased distant TFR slope would be $a = -6.09 \pm 0.28$. Assuming a 3 $\times$ larger scatter than locally we found a debiased distant slope of $a = -7.64 \pm 0.27$. However, the local TFR is *also* affected by a magnitude limit. The debiased local TF bisector fit slope we find is $a = -8.02 \pm 0.41$ (of course, the unchanged local TF scatter of $\sigma_B = 0.41$ mag was used here). We hence conclude that the distant and local TFR would be consistent in terms of an incompleteness effect only *if the TF scatter evolved by more than a factor of 3 over the past* $\sim$5 Gyr. This would be in agreement with the observed distant scatter, which is $\sigma_B \approx 1.2$ mag. On the other hand, this might be an overestimate since the free-fit scatter (i.e., with a slope $a = -4.27$, see the beginning of § 5) is only $\sim$0.9 mag.

These results imply that the differences between the distant and local TF distributions can at least in part be attributed to an incompleteness effect. However, the TFR directly traces only the overall luminosities of a galaxy sample, not the properties of the stellar populations. To perform a more detailed analysis, we converted the rest-frame, absorption-corrected $B - R$ colors of the galaxies in our sample into K-band M/L following Bell & de Jong (2001). In Figure 3, we show the M/L_K versus measured K-band absolute magnitudes of the distant TF spirals in comparison to local disk galaxies. We have split the distant galaxies into two redshift bins covering $z < 0.45$ (*filled symbols*) and $z > 0.45$ (*open symbols*). It is evident that the distant TF galaxies on the average have lower mass-to-light ratios at a given luminosity than their present-day counterparts (*shaded area*; note that several of the distant galaxies are at the *upper* limit of the local distribution, indicating that our selection did not miss disks with high M/L).

Moreover, there is a dependency on luminosity: low-luminosity galaxies seem to evolve stronger in M/L_K than high-luminosity galaxies. One possible explanation for this could be a larger fraction of young stars in the distant low-luminosity galaxies than high-luminosity galaxies. Since the K-band luminosity is a good tracer of stellar mass, this would imply higher luminosity-weighted stellar ages toward higher stellar masses.

For comparison, we also computed the luminosities and mass-to-light ratios of the disk galaxies that were not included in the TF sample due to kinematic disturbances, low S/N of their emission lines, or lack of significant rotation. These galaxies are shown in Figure 4, divided into two z bins as in Figure 3. The non-TF galaxies show a similar trend as the distant TF spirals, i.e., a stronger evolution of the M/L in the low-luminosity regime with respect to the high-luminosity regime. Note that there is no evidence for very blue, luminous disk galaxies that have been excluded from the TF analysis (in principle, such a population of luminous disks with blue colors and irregular kinematics could be expected within the framework of the hierarchical scenario, e.g., due to high-mass spirals that have recently undergone merger events).

Could the observed evolution of the M/L indicate a difference in stellar ages between high- and low-luminosity disks in the distant universe? Indeed, this interpretation gains support from an analysis of the broadband colors of galaxies at $z > 0.5$ from our data set with single-zone models of chemical enrichment, which yielded evidence for a dependence of the mean stellar ages on $V_{\max}$ (and hence total mass): the high-mass galaxies have older stellar populations than the low-mass ones (see Ferreras et al. 2004). This indication for an antihierarchical evolution of the baryonic component of galaxies ("downsizing") has also been found in other studies of distant galaxies (e.g., Kodama et al. 2004; van der Wel et al. 2005). It is possible that the various evolutionary effects coming into play between the earlier and the local universe—the evolution of the stellar populations, gas mass fractions, dust content, etc.—balance each other in such a way

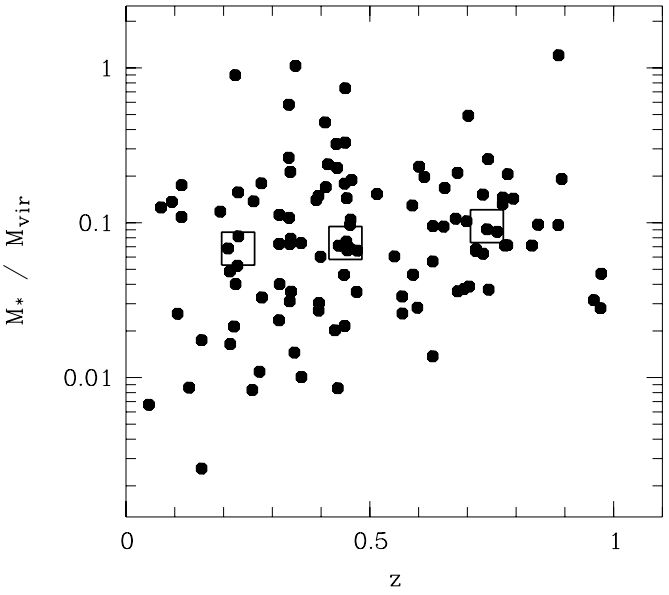

FIG. 5.—Stellar-to-total mass fractions of the 110 galaxies from our sample with determined V_{max} and available K-band photometry. The three large open squares show the median mass fraction within three redshift bins containing 36–37 galaxies each. The lack of a stellar mass fraction increase toward lower redshift favors a hierarchical buildup of the galaxies (see text for details). [*See the electronic edition of the Journal for a color version of this figure.*]

that the downsizing phenomenon is *not* reflected in a significant differential evolution of the Tully-Fisher relation.

The lack of hierarchical evolution in terms of the stellar populations raises the question whether a hierarchical evolution of the dark matter halos—the most fundamental prediction of (Λ)CDM cosmology—can be established with the data. To test this, we will use an approach similar to that of Conselice et al. (2005) by focussing on the evolution of the ratio between stellar and total mass since redshift $z = 1$. Based on the K-band mass-to-light ratios, we transformed the absolute K magnitudes into stellar masses M_*. Total masses were estimated from the disk scale lengths and maximum rotation velocities, adopting the results of van den Bosch (2002). Our sample covers the ranges of $2.0 \times 10^8\ M_\odot < M_* < 3.7 \times 10^{11}\ M_\odot$ (median $\langle M_* \rangle = 9.0 \times 10^9\ M_\odot$) in stellar mass and $2.5 \times 10^9\ M_\odot < M_{vir} < 5.2 \times 10^{12}\ M_\odot$ (median$\langle M_{vir} \rangle = 1.1 \times 10^{11}\ M_\odot$) in total mass.

In Figure 5, we show the ratio between stellar and total mass as a function of redshift. If we subdivide our sample into three redshift bins with 36 to 37 galaxies in each bin, we find median stellar mass fractions of 0.068, 0.074, and 0.095 at redshifts $z < 0.35$, $0.35 < z < 0.6$, and $z > 0.6$, respectively. We hence observe a very slight decrease of the stellar mass fraction of spirals between $z = 1$ and the local universe. If late-type galaxies contained all their gas by redshift unity and only converted gas into stars since then, an increase of the stellar mass fraction would be the result. Instead of such a "monolithic" scenario, which is reliable to describe the evolution of massive ellipticals, the data indicate that spiral galaxies have accreted baryonic (and most probably also dark) matter in the regime $0 < z < 1$, in agreement with the observational findings of Conselice et al. (2005) and with the expectation for a hierarchical structure growth (e.g., Baugh et al. 2005).

6. CONCLUSIONS

We have used VLT/FORS spectroscopy and *HST*/ACS imaging to construct a sample of 220 field spiral galaxies up to redshift $z = 1$. Spatially resolved rotation curves were extracted and fitted with synthetic velocity fields that take into account all geometric and observational effects, like blurring due to the slit width and seeing influence. Using these fits, the maximum rotation velocity V_{max} could be determined for 124 galaxies with an average lookback time of $\sim$5 Gyr. We find that this sample is offset from the local Tully-Fisher relation. The distant low-mass galaxies are more luminous at given V_{max} than their local counterparts, whereas the distant high-mass spirals are compatible with the local TFR. Taking the magnitude limit of our sample into account, we show that the slope of local and distant relation would be in compliance if the TFR scatter decreased by more than a factor of 3 between $z \approx 0.5$ and 0. On the other hand, the M/L indicate a luminosity-dependent evolution in the sense that distant low-luminosity disks have much lower M/L than their local counterparts, while high-luminosity disks barely evolved in M/L over the covered redshift range. This could be interpreted as an indication of the "downsizing" effect, i.e., the successive shift of star formation from high-mass to low-mass galaxies toward lower redshifts. In terms of the dark matter halos, we find evidence for a hierarchical evolution, since the fraction between stellar and total mass remained roughly constant since $z = 1$.

We thank ESO for the efficient support during the spectroscopic observations and the FDF team for the contributions to the FDF sample analysis. We also thank the anonymous referee for the comments and suggestions, which helped to significantly improve the paper. We are furthermore grateful to J. Fliri and A. Riffeser (both USM München) for the cosmic ray removal on the ACS images of the FDF and J. Heidt (LSW Heidelberg) for providing WHDF pre-images. This work was funded by the Volkswagen Foundation (I/76 520) and the "Deutsches Zentrum für Luft- und Raumfahrt" (50 OR 0301).

REFERENCES

Abadi, M. G., Navarro, J. F., Steinmetz, M., & Eke, V. R. 2003, ApJ, 591, 499
Bahcall, N., Ostriker, J. P., Perlmutter, S., & Steinhardt, P. J. 1999, Science, 284, 1481
Bamford, S. P., Aragon-Salamanca, A., & Milvang-Jensen, B. 2006, MNRAS, 366, 308
Baugh, C. M., Lacey, C. G., Frenk, C. S., Granato, G. L., Silva, L., Bressan, A., Benson, A. J., & Cole, S. 2005, MNRAS, 356, 1191
Bell, E. F., & de Jong, R. S. 2000, MNRAS, 312, 497
———. 2001, ApJ, 550, 212
Bender, R., et al. 2001, in Deep Fields, ed. S. Christiani, A. Renzini, & R. E. Williams (Berlin: Springer), 96
Böhm, A., et al. 2004, A&A, 420, 97 (B04)
Boissier, S., & Prantzos, N. 2001, MNRAS, 325, 321
Chiu, K., Bamford, S. P., & Bunker, A. 2007, MNRAS, 377, 806
Conselice, C. J., Bundy, K. E., Richard, S., Brichmann, J., Vogt, N. P., & Phillips, A. C. 2005, ApJ, 628, 160
Cowie, L. L., Songaila, A., Hu, E. M, & Cohen, J. G. 1996, AJ, 112, 839
Ferreras, I., & Silk, J. 2001, ApJ, 557, 165
Ferreras, I., Silk, J., Böhm, A., & Ziegler, B. L. 2004, MNRAS, 355, 64
Flores, H., Hammer, F., Puech, M., Amram, P., & Balkowski, C. 2006, A&A, 455, 107
Gabasch, A., et al. 2004, A&A, 421, 41
Giallongo, E., et al. 2005, ApJ, 622, 116
Giovanelli, R., et al. 1997, AJ, 113, 53
Heidt, J., et al. 2003, A&A, 398, 49
Kassin, S. A., et al. 2007, ApJ, 660, L35
Kodama, T., et al. 2004, MNRAS, 350, 1005
Metcalfe, N., Shanks, T., Campos, A., McCracken, H. J., & Fong, R. 2001, MNRAS, 323, 795

Milvang-Jensen, B., Aragón-Salamanca, A., Hau, G. K. T., Jørgensen, I., & Hjorth, J. 2003, MNRAS, 339, L1
Möller, C. S., Fritze-V. Alvensleben, U., Fricke, K. J., & Calzetti, D. 2001, Ap&SS, 276, 799
Nakamura, O., Aragón-Salamanca, A., Milvang-Jensen, B., Arimoto, N., Ikuta, C., & Bamford, S. P. 2006, MNRAS, 366, 144
Peng, C. Y., Ho, L. C., Impey, C. D., & Rix, H.-W. 2002, AJ, 124, 266
Pierce, M. J., & Tully, R. B. 1992, ApJ, 387, 47 (PT92)
Portinari, L., & Sommer-Larsen, J. 2007, MNRAS, 375, 913
Spergel, D. N., et al. 2003, ApJS, 148, 175
Steinmetz, M., & Navarro, J. 1999, ApJ, 513, 555
Tully, R. B., & Fouqué, P. 1985, ApJS, 58, 67
Tully, R. B., et al. 1998, AJ, 115, 2264
van den Bosch, F. C. 2002, MNRAS, 332, 456
van der Wel, A., Franx, M., van Dokkum, P. G., Rix, H.-W., Illingworth, G. D., & Rosati, P. 2005, ApJ, 631, 145
Vogt, N. P. 2001, in Deep Fields, ed. S. Cristiani, A. Renzini, & R. E. Williams (Berlin: Springer), 112
Weiner, B., et al. 2006, ApJ, 653, 1049
Ziegler, B. L., Böhm, A., & Fritz, A. 2006, EAS, 20, 303
Ziegler, B. L., Thomas, D., Böhm, A., Bender, R., Fritz, A., & Maraston, C. 2005, A&A, 433, 519
Ziegler, B. L., et al. 2002, ApJ, 564, L69